

Jerzy ŚWIDER
Adrian ZBILSKI

POWER LOSSES AND THEIR PROPERTIES FOR LOW RANGE OF A ROBOT ELECTRIC MOTOR WORKING CONDITIONS AS THE PART OF ENERGY EFFECTIVENESS RESEARCH

STRATY MOCY ORAZ ICH WŁASNOŚCI W NISKIM ZAKRESIE WARUNKÓW PRACY SILNIKA ELEKTRYCZNEGO ROBOTA W KONTEKŚCIE BADAŃ EFEKTYWNOŚCI ENERGETYCZNEJ*

Power losses are one of many factors affecting the energy effectiveness of production processes, however despite this, commonly investigated ranges of power losses do not explain how they change in the stages being different from a typical driving mode. This investigation focuses on low working conditions of a robot electric motor and the properties of power losses changes while going from a driving mode into a stand-still mode of electric motor work. Apart from determined values of power maps components, this work shows how to manage with technical limitations in performing measurements of industrial robot electrical states at the industrial conditions, like high disturbances, noise and limited range of robot axis angle position.

Keywords: energy effectiveness, industrial robot, electric motor, power maps, power losses, disturbances, noise, harmonics.

Straty mocy są jednym z wielu czynników wpływających na efektywność energetyczną procesów produkcyjnych, jednak pomimo tego, najczęściej badane zakresy strat mocy nie określają sposobu ich zmian w trybach pracy odmiennych od typowej pracy napędowej. Opisane badania zostały skoncentrowane na niskim zakresie warunków pracy silnika robota przemysłowego oraz na własnościach zmian postaci strat mocy podczas przechodzenia ze stanu pracy napędowej do pracy statycznej. Oprócz wyznaczonych wartości komponentów map mocy, w pracy przedstawiono techniczne rozwiązania umożliwiające wykonywanie pomiarów stanów elektrycznych robota w warunkach przemysłowych, którymi były zniekształcenia, zakłócenia oraz ograniczony zakres pozycji kątowych badanego przegubu robota.

Słowa kluczowe: efektywność energetyczna, robot przemysłowy, silnik elektryczny, mapy mocy, straty mocy, zniekształcenia, zakłócenia, harmoniczne.

1. Introduction

Energy effectiveness of a production processes is a part of a machines building and exploitation discipline, whose significance was already noticed and is constantly being developed [3, 4, 9, 10, 11]. Authors of this paper focused an attention in their work on all factors, having an influence on the final electrical energy, consumed by the manipulation and transportation machines and particularly consumed by industrial robots.

This investigation is an extension of the work with power losses in the FANUC AM100iB robot electric motors, presented in [20], and introduces some partial improvement into a wider energy effectiveness research.

The object of this investigation was a Fanuc AM100iB robot (Fig. 1), and more specifically its first electrical motor – working at steady-state at low range conditions, that are low speed and under low load. Because the robot motors are powered by a power electronic amplifier, a significant power distortion and noise, produced by a diodebridge rectifiers and PWM technology, an internal inaccuracies, electrical unbalances or system nonlinearities such as transformer saturation had to be included [7, 12].

The limitation this work has to faced with, was a necessity to keep the investigated motor being connected to the original amplifier as the



Fig. 1. General view of the investigated Fanuc AM100iB robot

only one available power source and a control unit. Simultaneously significantly distorted electrical voltages waveforms caused high values fluctuations and the motor shafts could rotate only in a limited range because of an original robot control unit safety systems. As a

(*) Tekst artykułu w polskiej wersji językowej dostępny w elektronicznym wydaniu kwartalnika na stronie www.ein.org.pl

consequence the steady-states had to be recognised and analysed in a separate off-line mode. This circumstance and requirements reconstructed real exploitation conditions and can explain what measurement equipment and measurement attitude had to be considered to achieve reliable results.

In order to properly determine electrical power values for low range conditions, the proper measurement methods for noise and distorted waveforms had to be considered. From among of many known power calculation solutions, allowing for considering high disturbances, the IEEE 1459-2010 standard [8] has been chosen. The selection was affected by a pragmatic oriented goals, which were possibilities to keep the results being mostly comparable with measurements, performed by currently manufactured power analysers [6]. The most common alternative power calculation methods proper for unbalanced systems, nonsinusoidal, disturbed and noised conditions and mainly used for scientific works are Budeanu's, Fryze's and Czarniecki's methods [1, 5, 15, 18, 19].

2. The goals of investigations

The all of robot dynamical parameters are ones of its many properties, which affect the energy effectiveness of its work. In this research case, the attention was focused on identifying the power losses in the first electrical motor for the low range working conditions, particularly for low speed and low load range. A separate cognition of the electrical properties behavior while going from a driving work mode into a stand-still mode was cared about. Moreover, also those signal processing techniques

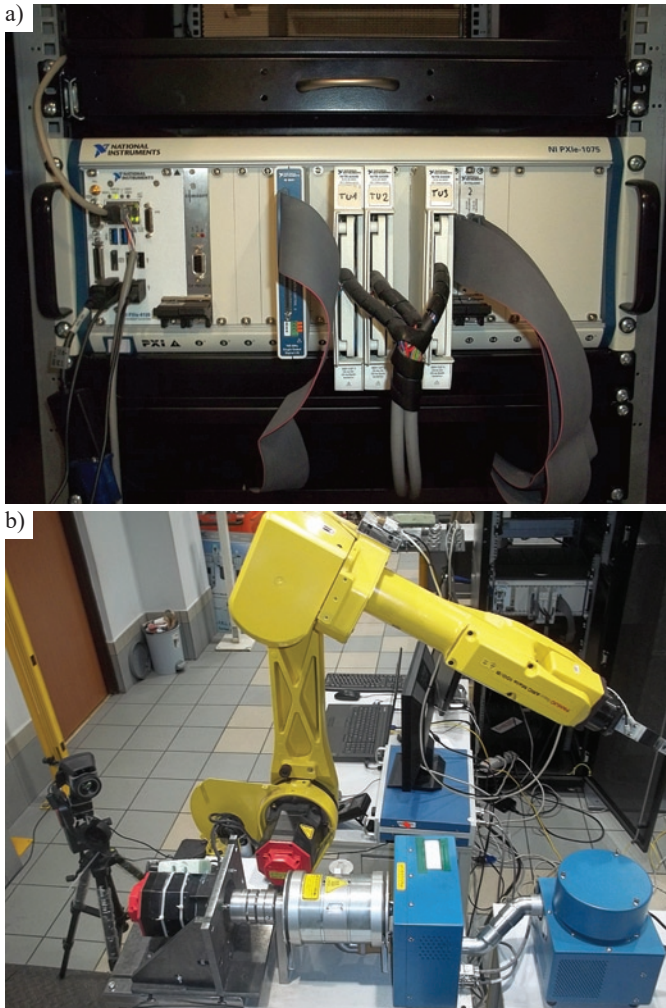


Fig. 2. a) NI PXIe-1075 system with measurement cards; b) General view of the investigated robot electric motor

were evaluated, which the measurement utilities could be extended by, in order to automatise measurement processes.

3. Measurement equipment

For performing an electrical power analyses and for acquisition of the kinematic parameters of the investigated FANUC AM100iB robot, the specialised measurement equipment was designed and built up (Fig. 2a). The apparatus consisted of NI 6581, NI 3xTB-4300B and 2x NI PXIe-6363 cards allowed for high frequency sampling of the electrical voltage and current waveforms in all power lines and for monitoring and decoding digital data containing shafts angle positions, generated by the *FANUC Pulse Coders*. However, the alternative solution for determining kinematic parameters of electric motors shafts

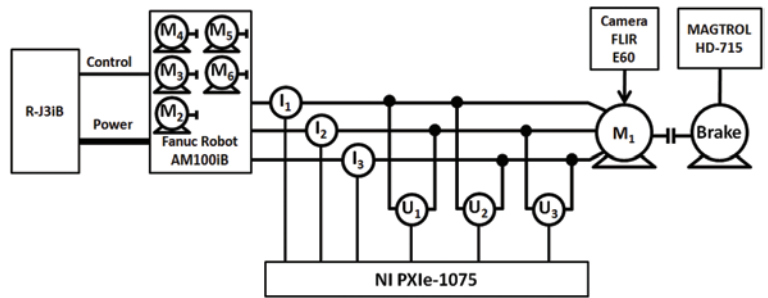


Fig. 3. Wiring diagram

by a direct measurement of a robot arm angle positions - available to recalculate into shafts' angle positions, could also be considered and is widely described in the following paper [13] for TCP robot point. The all acquisition devices were synchronised and controlled by a NI PXIe-1075 system and the LabVIEW SCADA application. The mechanical load of motor shaft and mechanical power was created and measured by the hysteresis brake MAGTROL HD-715 (Fig. 2b).

The wiring diagram and the mechanical connection scheme is shown in Fig. 3. The example raw data for an electrical voltage and current waveforms collected by this equipment show the graphs in Fig. 4. The specimen of the recorded signal is designated by the black fat line, which simultaneously indicates the rms value. The signals waveforms shapes result from the limited range of an angle position the motor shaft was able to rotate.

The longer recording duration of the specimen in steady-state, the most accurately the disturbances and noise were reduced from the final power calculation and the better final quality was achieved. Mainly the specimen's recording duration influenced on the fundamental harmonic frequency identification correction from the value numerically identified by FFT analysis. Additionally the longest specimen's recording duration, the more accurate angle phases shifts between electrical voltages and currents were recognised. From the other site, the maximum specimen's recording duration was limited by the limited range of an available angle rotation.

The wiring temperature was monitored in an indirect measurement by the use of the FLIR E60 thermographic camera. The all measurements were performed for the circumstances when the motors cover's temperature was in the range between 42-48°C (Fig. 5).

4. Power calculation

The distortion and noise level in an electrical voltage and current waveforms is evaluated by the index called the total harmonic distortion (THD), which according to IEEE 519-1992 is defined as the ratio of the rms of the harmonic content to the rms of fundamental quantity and is expressed as a percent of the fundamental harmonic [17]. The total harmonic distortions – THD, for an electrical voltage and cur-

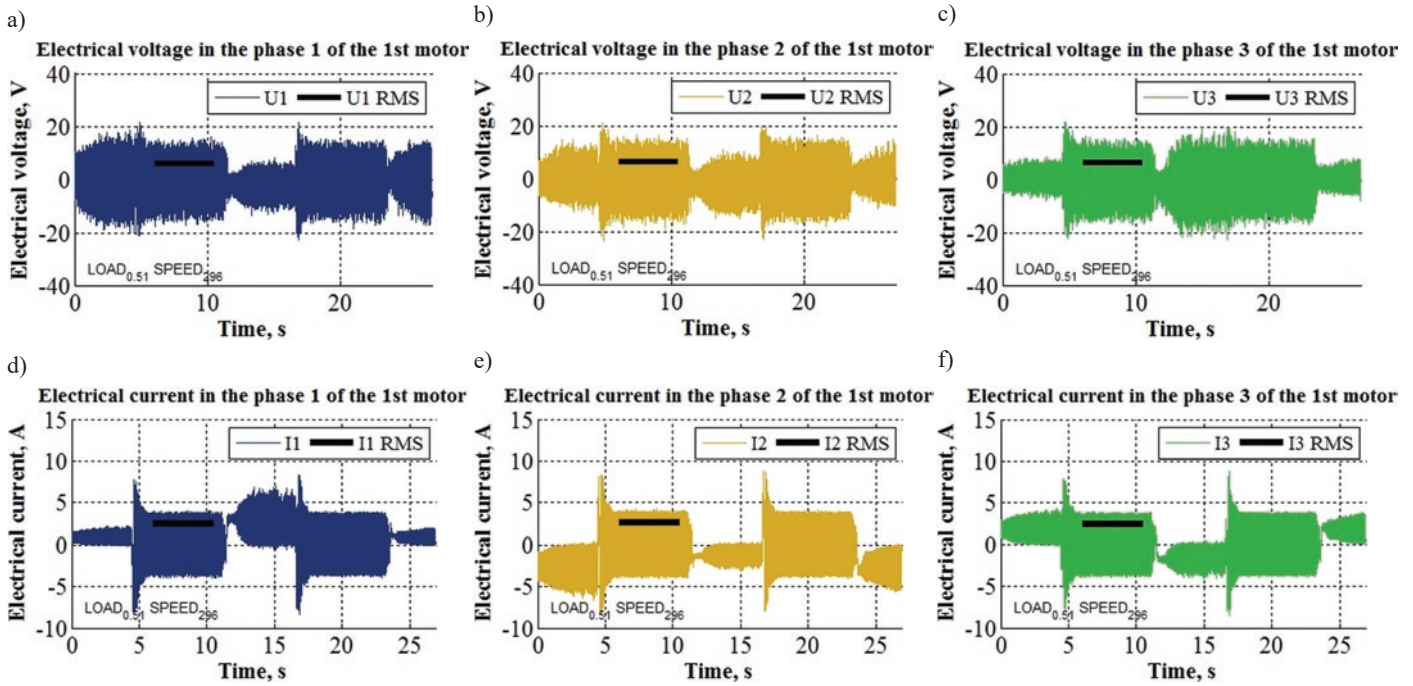


Fig. 4. Raw data

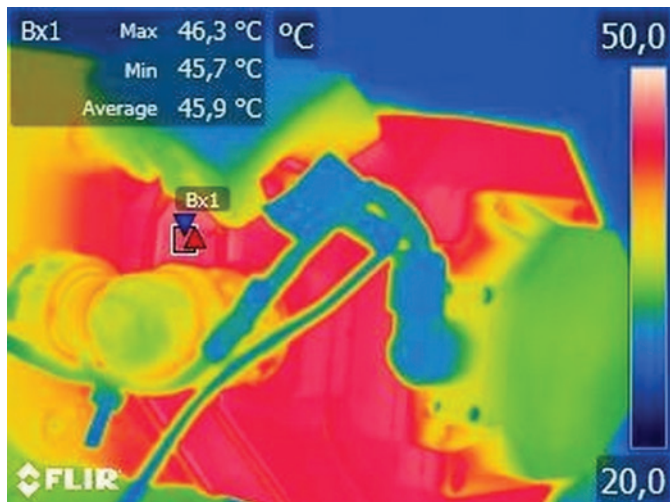


Fig. 5. Thermographic view of the electric motor cover

rent, in an accordance with the newest standard [7, 8] are expressed respectively by the equations (1) and (2):

$$THD_V = \frac{\sqrt{\sum_{k=2}^{\infty} V_{krms}^2}}{V_{1rms}} \cdot 100\% \quad (1)$$

$$THD_I = \frac{\sqrt{\sum_{k=2}^{\infty} I_{krms}^2}}{I_{1rms}} \cdot 100\% \quad (2)$$

V_{krms} and I_{krms} mean an rms value of respectively harmonic components of an electrical voltage and electrical current noise, V_1 and I_1 mean an rms value of respectively a fundamental harmonic of electrical voltage and electrical current values.

In electrical grids working with frequencies 50/60 Hz the most significant harmonics affecting the measurements are the 3rd, 5th and 7th [7]. However, because the fundamental frequencies, the number of significant harmonic components and their values varied in a wide

range and changed in different working conditions, therefore instead of a pure harmonic distortion measurement the combined total harmonic distortion plus noise method (THD+N) for determining the values of THD_V and THD_I was finally used (3) [2, 14, 16, 22]:

$$THD + N = \frac{\sum_{n=2}^{\infty} (S_{harm} + S_{noise})_{rms}}{S_{rms}} \quad (3)$$

S_{harm} means the value of an electric voltage or current harmonic distortion, S_{noise} means the value of an electric voltage or current harmonic noise and S_{rms} represents the rms value of a total electric voltage or current waveform.

To determine the fundamental electric voltage and electric current harmonics frequencies and to determine their magnitudes values and to evaluate their quality, the Fast Fourier Transform - FFT and a pattern sinusoidal signals were used. Pattern sinusoidal signals were manually tuned to the analysed waveforms, extracted from the measured signals (4) and used for determining the proper sample index, which the specimens had to begin from. They were also used for determining a phase shifts between electrical voltage and current waveforms. Additionally the pattern signals were used for the correction of the fundamental frequencies values recognised by FFT if that was required. The waveforms of measured parameters became the waveforms of the total distortion and noise signals after extracting the fundamental signal harmonics from them (5). The resultant normalised distortion, noise and fundamental harmonic waveforms are shown in Fig. 6.

$$S_1 = S - S_p \quad (4)$$

$$\sum_{n=2}^{\infty} S_{harm} + S_{noise} = S - S_1 \quad (5)$$

The example spectrum analyses of electrical voltage and current waveforms for low working condition range are shown in Fig. 7. Based on the graphs in Fig. 6 and Fig. 7 the rms of total

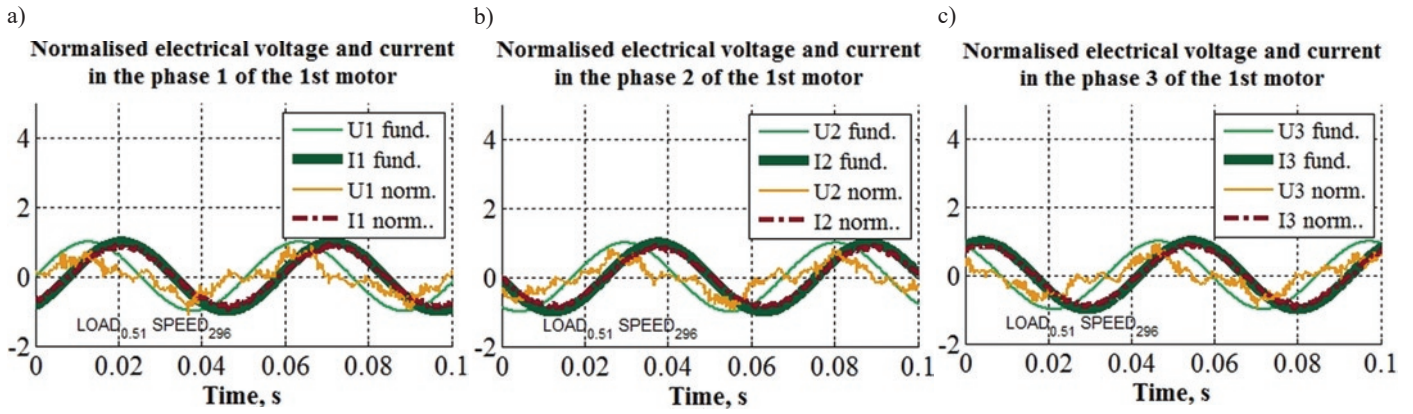


Fig. 6. Normalised electrical voltage and current waveforms and sinusoidal patterns of their fundamental harmonics in each phase of the 1st robot motor

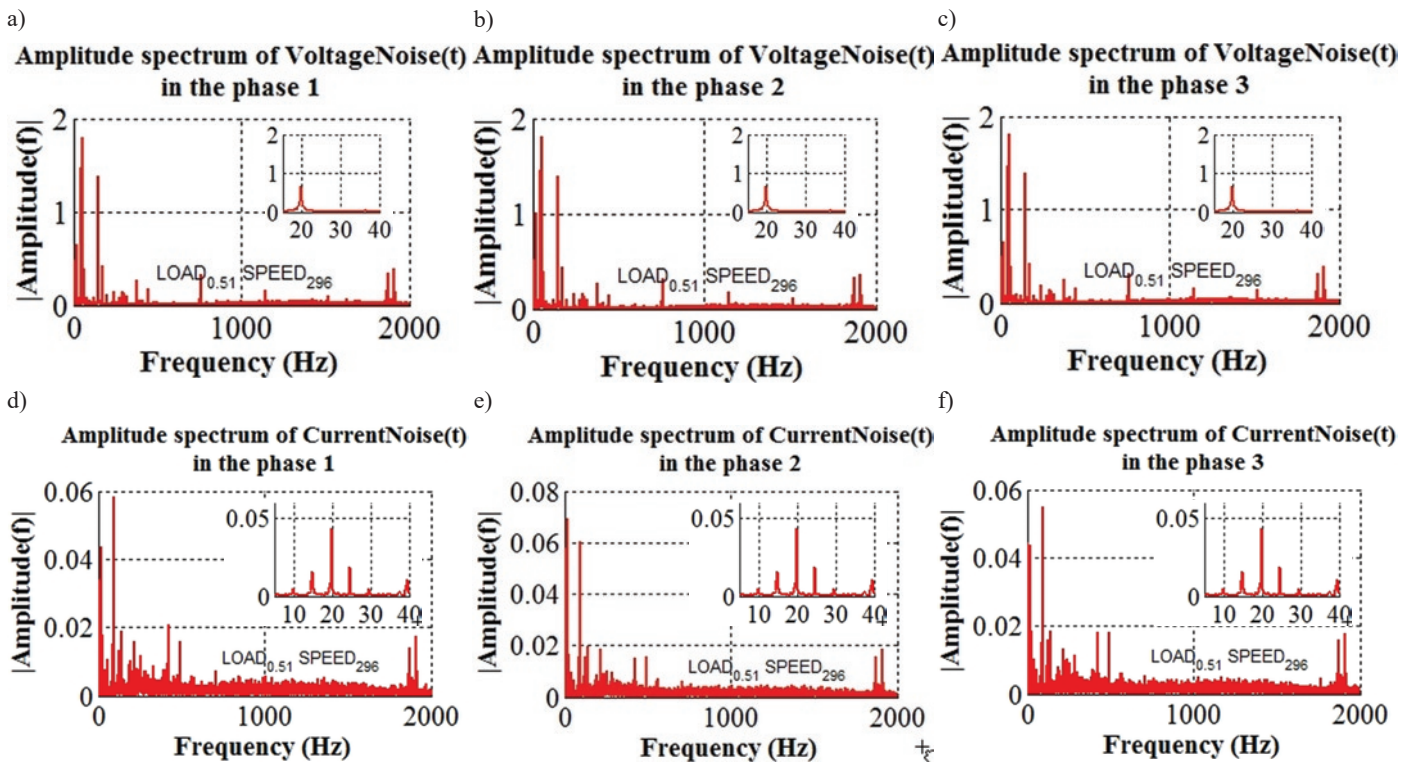


Fig. 7. Spectrum analyses for electrical voltage and current waveforms. In the top right corners the reduced fundamental harmonics are shown

disturbances and noise waveforms, the fundamental frequencies and their amplitudes were identified as well as the quality of disturbances and noise reduction was evaluated. The example relation between disturbances, noise and fundamental frequencies are shown in Fig. 8.

An electrical active power in each phase, measured by a 3V3A/ Three-voltage three-current method [23], used for three-wire systems and line-to-line nonsinusoidal, unbalanced cases was calculated by (6), (7), (8) [8]:

$$P_A = V_A \cdot I_A \cdot PF_{True A} \quad (6)$$

$$P_B = V_B \cdot I_B \cdot PF_{True B} \quad (7)$$

$$P_C = V_C \cdot I_C \cdot PF_{True C} \quad (8)$$

V_A , V_B and V_C mean an rms value of an electrical voltage in the phase A , B and C respectively, I_A , I_B and I_C mean an rms value of an

electrical current in the phase A , B and C respectively, P_A , P_B and P_C mean an electrical power in the phase A , B and C respectively, PF_{true} means true power factor (9), consisted of PF_{disp} - displacement power factor (10) and PF_{dist} - distortion power factor (11) like in [7, 8]:

$$PF_{true} = PF_{displ} \cdot PF_{dist} \quad (9)$$

$$PF_{displ} = \cos(\delta - \theta) \quad (10)$$

$$PF_{dist} = \frac{1}{\sqrt{1 + (THD_V / 100)^2} \cdot \sqrt{1 + (THD_I / 100)^2}} \quad (11)$$

where δ and θ mean voltage and current phase shifts respectively, THD_V and THD_I mean electrical voltage and current distortion and noise respectively.

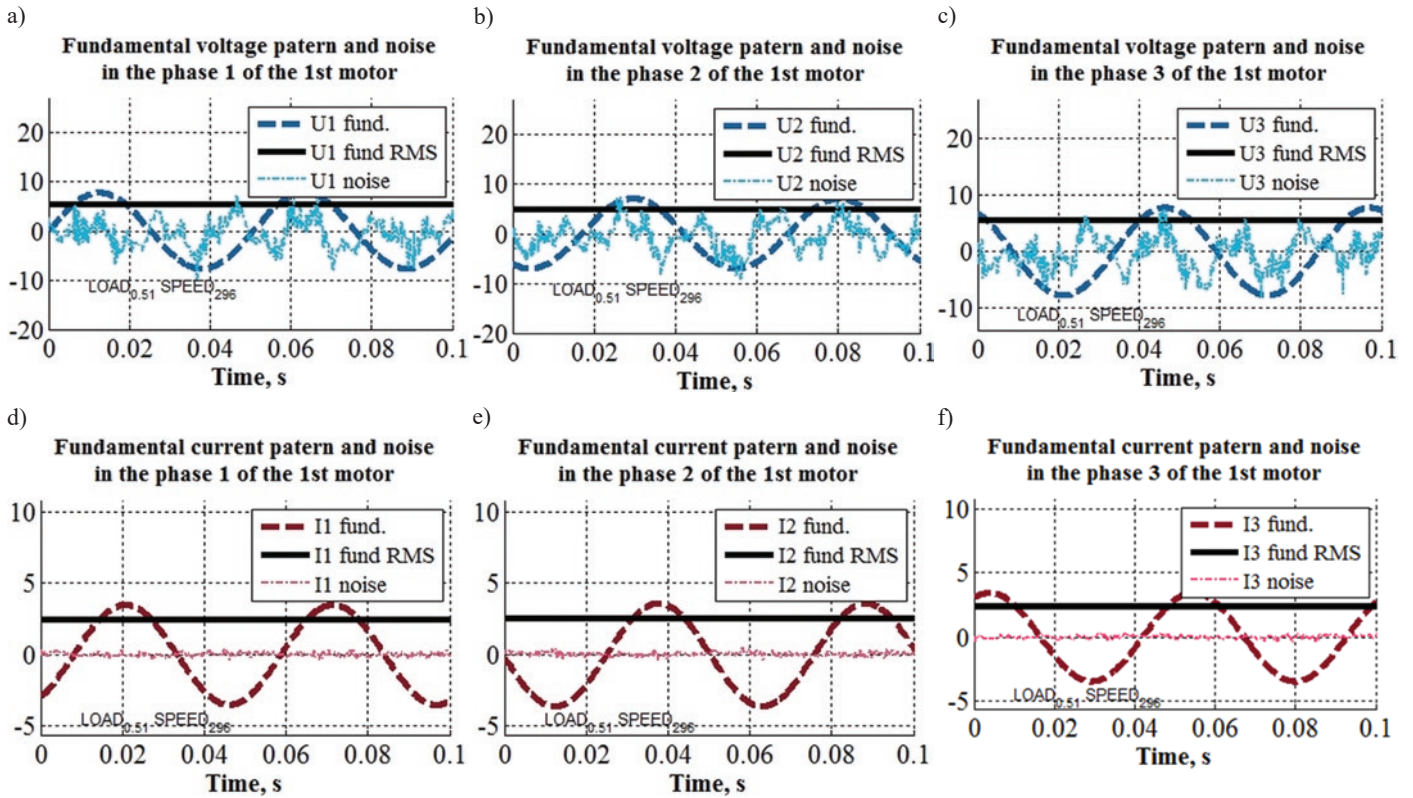


Fig. 8. Example of distortion, noise and fundamental harmonics waveforms comparison for low working conditions

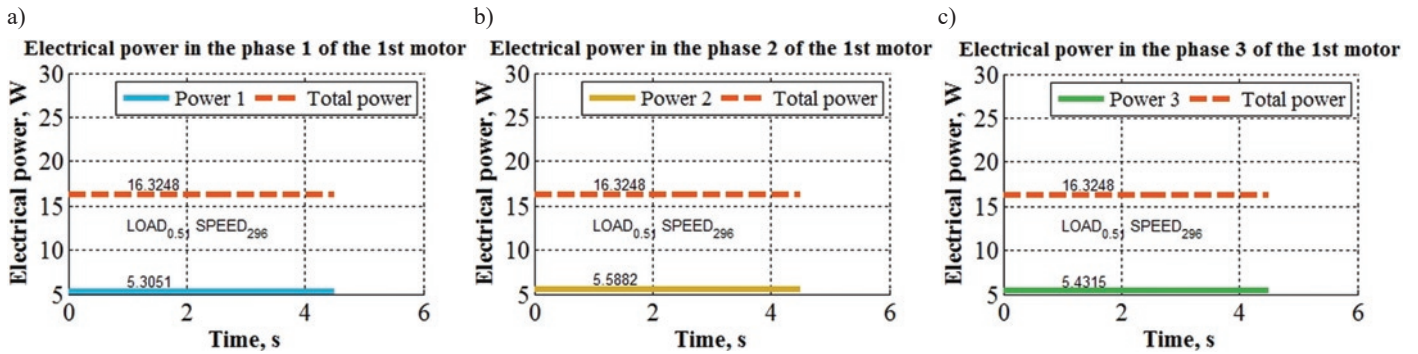


Fig. 9. Selected results for a total electrical power and electrical power in each phase for low working conditions

The total active electrical power was calculated by the equation (12) (Fig. 9), inter alia used for the three-wire *star* systems, for which the following balance $I_A + I_B + I_C = 0$ is true [8]:

$$P_T = P_A + P_B + P_C \quad (12)$$

The power losses map (13) (Fig. 10a) was calculated as a difference between the total active electrical power (12) (Fig. 10c) measured indirectly by the NI PXIe-1075 system and the mechanical power (Fig. 10b) measured by the hysteresis MAGTROL HD-715 brake:

$$P_L(\tau_1, q_1) = P_T(\tau_1, q_1) - P_M(\tau_1, q_1) \quad (13)$$

The energy efficiency map was calculated as the ration between input and output power (14) (Fig. 10d):

$$(\tau_1, q_1) = \frac{P_M(\tau_1, q_1)}{P_T(\tau_1, q_1)} \quad (14)$$

Because of its comprehensive range of information, the power losses map (Fig. 10a) is the most significant input data for modelling electrical power losses, being the part of the total energy consumption, evaluated in energy effectiveness analysis of industrial production processes performed by investigated robot [20, 21, 24].

Performed investigations showed that the change of electrical states while changing work from the driving into stand-still mode is very abrupt, and in the case of investigated motor takes places between 0 and 6 rpm (Fig. 11). Additionally there is also a visible gap above 6 rpm, recorded for every load case (Fig. 11). Those facts have to be included in the numerical robot model being under development by the authors of this paper.

5. Conclusion

The measurement equipment was a proper selection for managing with the limitations and accuracy level requirements resulted from necessity to keep the investigated electric motor being connected to the original control unit and resulted from low range working condition being under investigation. The apparatus allowed for recording a raw data with its harmonics up to very high frequencies and for providing

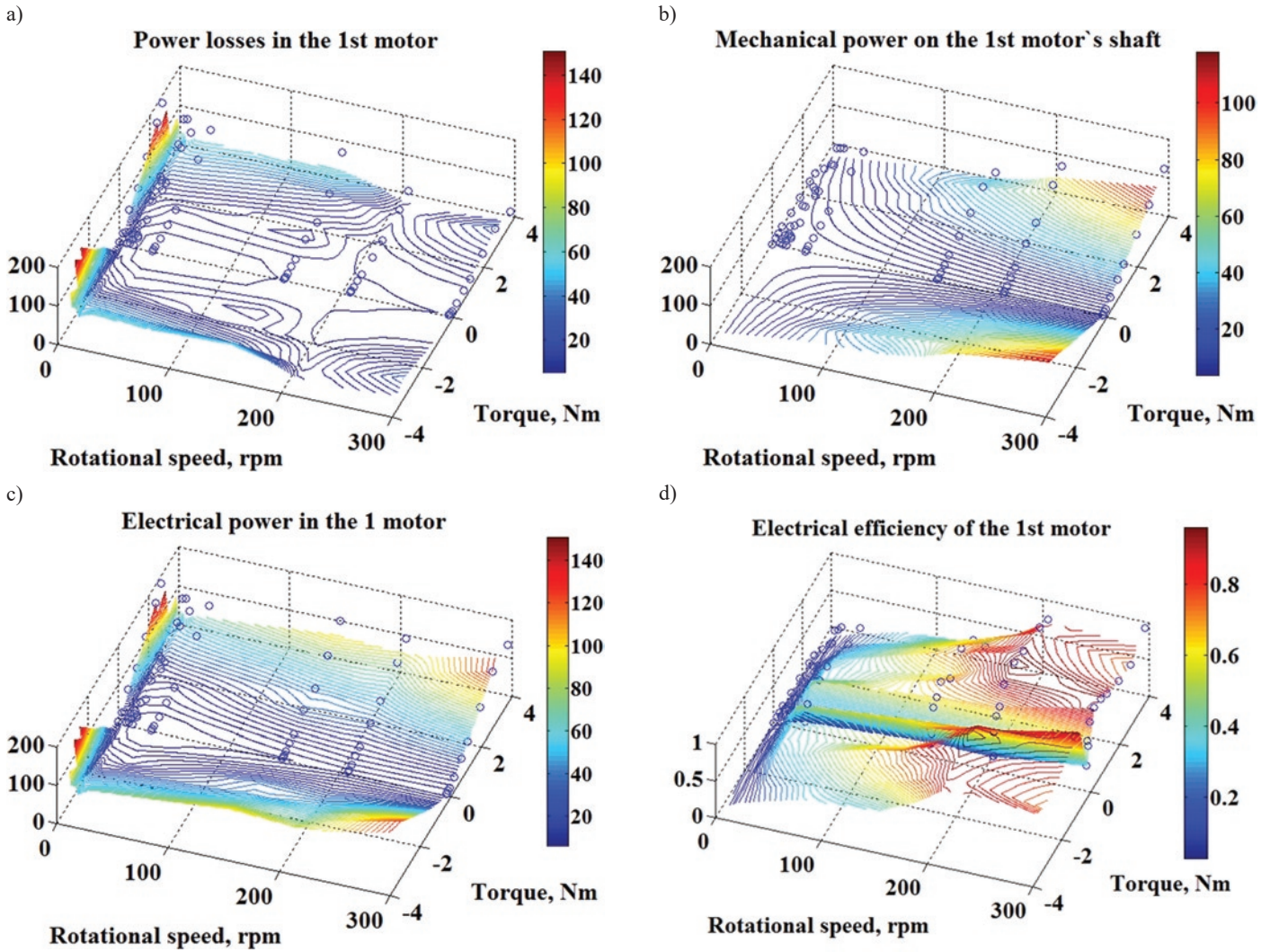


Fig. 10. Power maps for low working conditions

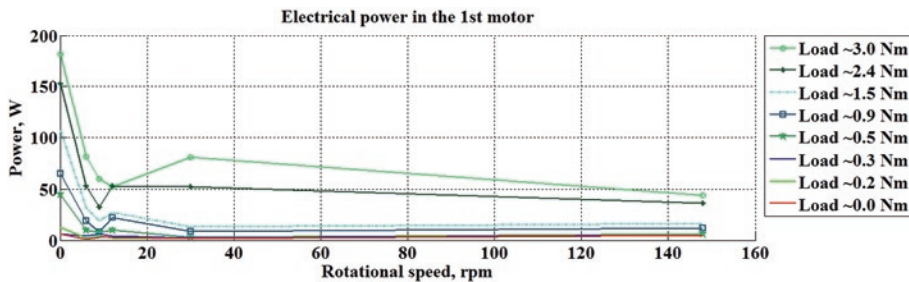


Fig. 11. Active electrical power in the 1st motor with visible abrupt electrical state change close to 6 rpm and with a gap above 6 rpm

high quality shaft's angle position. This solution could be compared to six power analysers working with extra feature to decode the digital data with values of kinematic parameters of the motor shafts.

Spectrum analyses showed that the pattern signals for notch filtering of sampled signals used for this work did not perfectly separate the fundamental harmonics from the disturbances and noise. As a consequence it extended a measurements uncertainty and decreased the final results' quality at a data processing stage. Nevertheless the level of already achieved reduction did not significantly influence on the results, what was evaluated by total power changes for more and more better reductions. Despite this the quality of band-stop filter for notch filtering of the fundamental harmonics application should be

evaluated yet and compared with so far used approach before further research of energy effectiveness.

Investigations of the low range working conditions showed that the electrical states between the driving mode and the stand-still mode change very abruptly and in the investigated motor case take place between 0 and 6 rpm and additionally there is a gap visible above 6 rpm, recorded for every load case.

Even more accurate investigation of the closest area of 6 rpm is required to avoid low resolution results and a total measurement uncertainty should be also evaluated in the further work.

The work has a cognitive significance, and its results explain which direction the further research should be focused on. Because an industrial robot is an example of highly non-linear system, therefore more unbalanced working conditions and higher nonlinear loads than those ones used and existed in this investigation must be expected in typical exploitation circumstances.

Acknowledgement

The project was financed from the funds of National Science Centre awarded on the basis of a decision number DEC-2011/03/B/ST8/04631.

References

1. Akagi H, Watanabe E H, Aredes M. Instantaneous Power Theory and Applications to Power Conditioning 2017: 27, <https://doi.org/10.1002/9781119307181>.
2. Audio Precision. More about THD+N and THD 2013.
3. Belda K, Burget P. Physical Modelling of Energy Consumption of Industrial Articulated Robots. 15th International Conference on Control, Automation and Systems (ICCAS 2015).
4. Brossog P M, Kohl J, Merhof J, Spreng S, Franke J. Energy Consumption and Dynamic Behavior Analysis of a Six-axis Industrial Robot in an Assembly System. CIRP 2014; 23: 131-136, <https://doi.org/10.1016/j.procir.2014.10.091>.
5. Bucci G, Ciancetta F, Fiorucci E, Ometto A. Survey about classical and innovative definitions of the power quantities under nonsinusoidal conditions. International Journal of Emerging Electric Power Systems 2017; 18(3): 1-16, <https://doi.org/10.1515/ijeeps-2017-0002>.
6. Fluke 434-II/435-II/437-II. Users Manual 2012. Rev.1 06/12.
7. Grady W M, Gilleskie R J. Harmonics and how they relate to power factor. Proc. of the EPRI Power Quality Issues & Opportunities Conference (PQA'93), San Diego, CA 1993: 3-10.
8. IEEE Standard Definitions for the Measurement of Electric Power Quantities Under Sinusoidal, Nonsinusoidal, Balanced, or Unbalanced Conditions. IEEE Std 1459TM-2010; (Revision of IEEE Std 1459-2000).
9. Liu A, Liu H, Yao B, Xu W, Yang M. Energy consumption modeling of industrial robot based on simulated power data and parameter identification. Advances in Mechanical Engineering 2018; 10 (5): 1-11, <https://doi.org/10.1177/1687814018773852>.
10. Mohammeda A, Schmidt B, Wanga L, Gaoc L. Minimizing Energy Consumption for Robot Arm Movement. Procedia CIRP 2014; 25: 400-405, <https://doi.org/10.1016/j.procir.2014.10.055>.
11. Paesa K, Dewulfa W, Elsta K V, Kellensb K, Slaetsa P. Energy efficient trajectories for an industrial ABB robot. CIRP 2014; 15: 105-110, <https://doi.org/10.1016/j.procir.2014.06.043>.
12. Park O S, Park J W, Bae C B, Kim J M. A Dead Time Compensation Algorithm of Independent Multi-Phase PMSM with Three- Dimensional Space Vector Control. Journal of Power Electronics 2013; 13 (1): 1, <https://doi.org/10.6113/JPE.2013.13.1.77>.
13. Płaczek M, Piszczek Ł. Testing of an industrial robot's accuracy and repeatability in off and online environment. Eksploatacja i Niezawodność - Maintenance and Reliability 2018; 20 (3): 455-464, <https://doi.org/10.17531/ein.2018.3.15>.
14. Rane. Audio specifications 2000; 2.
15. Revuelta P S, Litrán S P, Thomas J P. Active Power Line Conditioners: Design, Simulation and Implementation for Improving Power Quality 2015: 25.
16. Rhode&Schwarz. Harmonic Distortion Measurements in the Presence of Noise Application Note. June 17, 2011-0e.
17. Siemens. Harmonics in power systems, causes, effects and control 2013: 3.
18. Stevanović D, Petković P. A single-point method based on distortion power for the detection of harmonic sources in a power system. Metrology and Measurement Systems 2014; XXI (1): 3-14.
19. Szubert K. Power Measurement when waveform are distorted. Jakosc i uzytkowanie energii elektrycznej - Electrical Power Quality and Utilisation 1996; 2 (2);
20. Świder J, Zbilski A. Modelling of the power of losses in the Fanuc AM100iB robot drives and in its power electronic systems. Modelowanie inzynierskie - Engineering modeling 2013; 17(48): 138-142.
21. Świder J, Zbilski A. The modelling and analysis of a partial loads in the Fanuc AM100iB robot joints. International Journal of Modern Manufacturing Technologies 2013; V (2): 89-96.
22. Texas Instruments. Digital Audio Measurements 2001; SLAA114: p. 10.
23. Yokogawa. WT310/WT310HC/WT330 Digital Power Meter Getting Started Guide 2013: 2-25.
24. Zbilski A. Doctoral dissertation: Method for energy intensity analysis of manipulation and transportation processes 2014.

Jerzy ŚWIDER**Adrian ZBILSKI**

Silesian University of Technology

Faculty of Mechanical Engineering

Konarskiego St, 44-100 Gliwice, Poland

E-mails: jerzy.swider@polsl.pl, adrianzbilski@gmail.com
